Single-Phase Single-Stage Photovoltaic Generation System Based on a Ripple Correlation Control Maximum Power Point Tracking

Domenico Casadei, *Senior Member, IEEE*, Gabriele Grandi, *Member, IEEE*, and Claudio Rossi

***Abstract*—A maximum power point tracking algorithm for single-stage converters connecting photovoltaic (PV) panels to a single-phase grid is presented in this paper. The algorithm is based on the application of the "ripple correlation control" using as perturbation signals the current and voltage low-frequency oscillations introduced in the PV panels by the single-phase utility grid. The proposed control technique allows the generation of sinusoidal grid currents with unity power factor. The algorithm has been developed to allow an array of PV modules to be connected to the grid by using a single-stage converter. This simple structure yields higher efficiency and reliability when compared with standard solutions based on double-stage converter configurations.**

The proposed maximum power point tracking algorithm has been numerically simulated and experimentally verified by means of a converter prototype connected to a single-phase grid. The results are presented in the paper, showing the effectiveness of the proposed system.

***Index Terms*—Active filters, energy management, photovoltaic power systems, power conditioning, power quality.**

I. Introduction

PHOTOVOLTAIC (PV) technology is the most promising candidate for the large-scale adoption of a renewable energy source. Photovoltaic roofs represent an important share of new installations of PV panels. For these applications, the rated power is lower than 5 kW, and the PV panels are permanently connected to a single-phase grid. The power flow between the PV panels and the grid is controlled by a power conditioning system (PCS), which should be reliable and inexpensive. To obtain the maximum efficiency of the system, the PCS must keep the power extracted from the PV panels close to the maximum power point (MPP). Several solutions for a PCS with maximum power point tracking (MPPT) capability have recently been proposed, based on both single-stage [1] and double-stage converter topologies [2].

This paper deals with a single-phase, single-stage PCS configuration, employing a simple and effective MPPT embedded algorithm. The scheme of the proposed system is shown in Fig. 1. The output of the PV panels is directly connected to the dc link of the single-phase voltage source inverter (VSI), and the output of the inverter is connected to the grid through the ac link inductor $L_{\rm ac}$.

Manuscript received October 7, 2003; revised July 2, 2004. Paper no. TEC-00286-2003.

The authors are with the Department of Electrical Engineering, Alma Mater Studiorum-Università di Bologna, Bologna, Italy (e-mail: domenico.casadei@unibo.it; gabriele.grandi@unibo.it; claudio.rossi@unibo.it).

Digital Object Identifier 10.1109/TEC.2005.853784

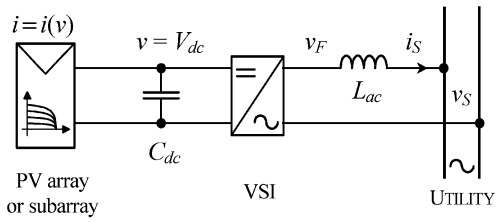

Fig. 1. Schematic diagram of the PV generation system.

II. Operating Principle

The VSI output voltage v_F is controlled in order to force the current injected into the mains i_S to follow a sinusoidal reference waveform, synchronized and in phase with the fundamental component of the source voltage v_S. As a consequence, a sinusoidal current is obtained even in the presence of voltage perturbations coming from the mains [3]. The amplitude of the reference source current I_S^* is generated by the dc link voltage regulator on the basis of the error between the dc link voltage $V_{\rm dc}$ and the reference dc voltage $V_{\rm dc}^*$ of the PV panels.

The MPPT algorithm varies $V_{\rm dc}^*$ according to the environmental conditions in order to keep the operating point of the PV panels close to the maximum power point.

The basic principle of the MPPT algorithm is to exploit current and voltage oscillations caused by the pulsations of the instantaneous power, which are inherent in single-phase power systems. Analyzing these oscillations allows us to obtain information about the power gradient and evaluate if the PV system operates close to the maximum power point.

It is known that for a non-null value of active power injected into a single-phase grid P_S, the instantaneous power $p_S(t)$ pulsates at a frequency twice than that of the grid. If the current $i_S(t)$ is in phase with the source voltage $v_S(t)$, the instantaneous value of power injected into the grid is

$$\begin{aligned} p_S(t) &= v_S(t) i_S(t) = \sqrt{2} V_S \cos \omega t \sqrt{2} I_S \cos \omega t \\ &= V_S I_S (1 + \cos 2\omega t). \end{aligned} \tag{1}$$

The average quantity $V_S I_S$ corresponds to the active power P_S. The power pulsation at the angular frequency 2ω in (1) is reflected on the dc link bus of the VSI as a voltage pulsation superimposed to the average of the dc link voltage $V_{\rm dc}$. The variation of $V_{\rm dc}$ can be related to active power P_S, grid angular frequency ω, and dc link capacitor $C_{\rm dc}$ by the following

relationship:

$$\frac{P_S}{\omega} = C_{\rm dc}\left(V_{\rm dcMAX}^2 - V_{\rm dcMIN}^2\right). \tag{2}$$

The dc link voltage excursion $(V_{\rm dcMAX} - V_{\rm dcMIN})$ can be limited by choosing a proper value for $C_{\rm dc}$, according to (2), ensuring the correct operation of the inverter. The residual oscillation of $V_{\rm dc}$ determines a small pulsation of the power supplied by the PV panels. On the basis of the phase relationship between power and voltage oscillations, the MPPT algorithm moves the operating point of the PV panels by varying $V_{\rm dc}^*$ until the MPP is reached. Voltage and current oscillations must be as small as possible in order to minimize the oscillation of power extracted from the panel. On the other hand, these oscillations must be large enough to be sensed and distinguished from current and voltage ripple due to the VSI switching effects. It has been observed that keeping voltage and current oscillation around 1% of their rated values leads to a good behavior of the whole PV generation system.

The capability of the proposed system to keep under control the power injected into the grid for any operating condition is ensured by the use of a reliable synchronizing device and an effective current regulator applied to the current injected into the grid. In particular, the synchronization of the inverter output voltages with the fundamental component of the source voltages is carried out by a phase-locked loop (PLL) control circuit. As a consequence, the proposed algorithm operates correctly even in presence of nonsinusoidal source voltages. The current regulator could be realized in different ways. In this paper, a predictive PWM current regulator has been utilized.

III. Analysis of the MPPT Algorithm

The aim of any MPPT algorithm is to extract the maximum power from the PV panels. Usually, the condition $\partial p/\partial v = 0$ is adopted to locate this operating point, since PV panels show a unique global maximum power point.

The MPPT algorithms are based on the determination of the slope of the PV panels output power versus voltage, i.e., the power derivative $\partial p/\partial v$. This quantity is utilized as representative of the "voltage error," i.e., the difference between the actual voltage of the PV panels and the reference voltage v^* corresponding to the maximum power operating point. The qualitative behavior of $\partial p/\partial v$ is represented in Fig. 2. In the region near v^*, the power derivative can be considered a straight line having the slope k.

In order to determine the power derivative $\partial p/\partial v$, it is necessary to introduce a voltage and current perturbation around any operating point of the PV array. Traditional MPPT algorithms are based on "perturbation and observation" method or "incremental conductance" method. Some variants to these methods have been presented in order to improve the dynamic performance and/or to reduce undesired oscillations around the MPP [1], [4], [5]. An alternative method is based on measuring and processing the current and/or voltage ripple due to the switching behavior of the converter connected to the PV panels array. This method is known as "ripple correlation control," first proposed in [7] and successively utilized in [8] and [9]. However, for small power PV generation systems, high switching frequency converters are usually adopted, reducing the residual voltage and current ripple below practical exploitable values.

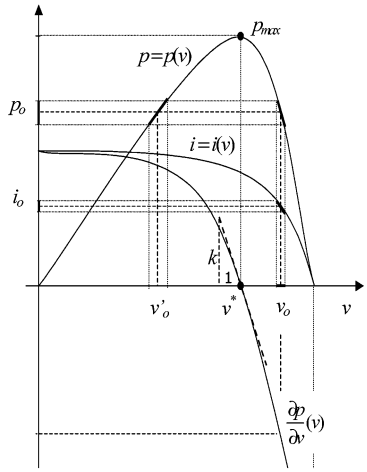

Fig. 2. Current, power, and power derivative of the PV panels versus voltage.

In order to overcome this problem, a MPPT algorithm is proposed in this paper, which is based on the application of the "ripple correlation control," using the double-frequency oscillation of the instantaneous power as perturbation signals. The oscillations of the instantaneous power are inherent in a single-phase PV system and can themselves be considered as embedded dynamic test signals useful in determining $\partial p/\partial v$. A key feature of this method is the knowledge of the oscillation period $T = 1/(2f)$ to improve the MPPT algorithm performance, where f is the grid frequency.

The application of the "ripple correlation control," combined with the use of the $2f$ power oscillation, can be considered the main contribution of this paper for improving the performance of single-phase PV systems. The basic principle will be described in more detail in the following. For this purpose, let us consider a periodic function $x(t)$ having the moving average component $\bar{x}(t)$ over the period T and the alternative component $\tilde{x}(t)$, defined, respectively, as

$$\bar{x}(t) = \frac{1}{T}\int_{t-T}^{t} x(\tau)\, d\tau \tag{3}$$

$$\tilde{x}(t) = x(t) - \bar{x}(t). \tag{4}$$

Applying these definitions to the output voltage and power of the PV panels leads to

$$v(t) = \bar{v}(t) + \tilde{v}(t) \tag{5}$$

$$p(t) = \bar{p}(t) + \tilde{p}(t). \tag{6}$$

The average operating point (v_o, p_o) on the $p = p(v)$ characteristic, and the corresponding voltage and power alternative components, are represented in Fig. 2, according to the following expressions:

$$\bar{p}(t) = p(\bar{v}(t)) = p(v_o), \quad \text{where } v_o = \bar{v}(t). \tag{7}$$

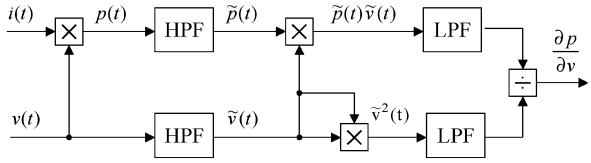

Fig. 3. Estimation of the PV power derivative by using filtering blocks.

Assuming the curve $p = p(v)$ is still valid for dynamic analysis [7] and linearizing the nearby average operating point $p_0 = p(v_0)$ leads to a simple relationship between the power ripple and the voltage ripple, which is expressed as

$$\tilde{p}(t) \cong \left(\frac{\partial p}{\partial v}\right)_{v_o} \tilde{v}(t). \tag{8}$$

The power derivative can be calculated by (8) as a function of power and voltage oscillations around the given operating point (v_o, p_o). In order to avoid critical calculations based on instantaneous power and voltage values as proposed in [9], it is possible to introduce, instead of (8), the moving average of the product of (8) and $\tilde{v}(t)$, leading to

$$\int_{t-T}^{t} \tilde{p}(\tau)\tilde{v}(\tau)\,d\tau \cong \left(\frac{\partial p}{\partial v}\right)_{v_o} \cdot \int_{t-T}^{t} \tilde{v}^2(\tau)\,d\tau. \tag{9}$$

Then, the power derivative can be evaluated as the following ratio:

$$\left(\frac{\partial p}{\partial v}\right)_{v_o} \cong \frac{\int_{t-T}^{t} \tilde{p}(\tau)\tilde{v}(\tau)\,d\tau}{\int_{t-T}^{t} \tilde{v}^2(\tau)\,d\tau}. \tag{10}$$

Note that in (10), the power derivative is expressed in terms of integral quantities and can be easy calculated.

The voltage and power alternative components utilized in (10) can be evaluated on the basis of (3) and (4), leading to

$$\tilde{v}(t) = v(t) - \frac{1}{T}\int_{t-T}^{t} v(\tau)\,d\tau \tag{11}$$

$$\tilde{p}(t) = p(t) - \frac{1}{T}\int_{t-T}^{t} p(\tau)\,d\tau. \tag{12}$$

Assuming the voltage and power oscillation frequency is known, a filtering approach can be usefully adopted to extract the alternative components of $p(t)$ and $v(t)$. In particular, highpass filters (HPFs) can be used instead of (11) and (12). In the same way, lowpass filters (LPFs) can be used instead of the moving averaging integrals of (10). The corresponding block diagram is depicted in Fig. 3. Using this method, it is possible to calculate the power derivative in a straightforward way, avoiding complicated and time consuming calculations.

The power derivative $\partial p/\partial v$ can be also used to represent the voltage error $\Delta v = v^* - v$, i.e., the difference between the MPP voltage and the actual voltage, since the relationship between power and voltage is almost linear in the region around the MPP, as shown in Fig. 2.

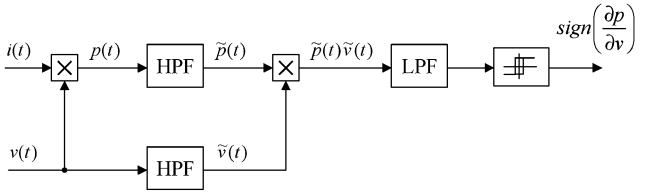

Fig. 4. Simplified estimation of the PV power derivative by using filtering blocks.

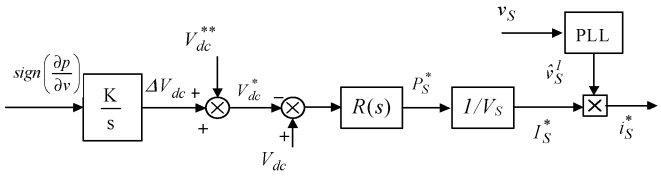

Fig. 5. DC-link voltage controller.

IV. Implementation of the MPPT Algorithm

The block diagram shown in Fig. 3 can be further simplified in order to be easily implemented on a low-cost digital signal processor, without reducing the performance of the MPPT algorithm. In particular, the average value of the product $\tilde{p} \cdot \tilde{v}$ could be conveniently utilized as the input variable of the dc link voltage regulator. In fact, on the basis of (9), since the integral on the right-hand side is always greater than zero, the sign of the integral on the left-hand side corresponds to the sign of the power derivative $\partial p/\partial v$:

$$\text{sign}\left(\int_{t-T}^{t} \tilde{p}(t)\tilde{v}(t)\,dt\right) = \text{sign}\left(\frac{\partial p}{\partial v}\right). \tag{13}$$

The quantity $\text{sign}(\partial p/\partial v)$ is a clear indication of the region where the PV panel is working:

- $(\partial p/\partial v) > 0$ means $\tilde{p}$ and $\tilde{v}$ are in phase agreement. The operating point is on the left side of the MPP on the $(I$–$V)$ characteristic.
- $(\partial p/\partial v) < 0)$ means $\tilde{p}$ and $\tilde{v}$ are in phase opposition. The operating point is on the right side of the MPP on the I–V characteristic.

The knowledge of the instantaneous operating point region makes it possible to change the dc link voltage reference in order to approach the maximum power operating point. On the basis of these considerations, the scheme of Fig. 3 can be simplified leading to scheme represented in Fig. 4, where only the quantity corresponding to the average value of the product $\tilde{p} \cdot \tilde{v}$ and its sign are computed. In particular, the sign is extracted by a hysteretic comparator, set by a small band around zero, with the output values $[-1, 1]$ representing $\text{sign}(\partial p/\partial v)$.

V. DC Link Voltage Controller

The scheme of the dc link voltage controller is represented in Fig. 5. When $\text{sign}(\partial p/\partial v) > 0$, the integrator increases its output ΔV_{dc}, and the dc link voltage reference V_{dc}^* moves toward the MPP. On the contrary, when $\text{sign}(\partial p/\partial v) < 0$, the integrator decreases ΔV_{dc}, and the dc link voltage reference V_{dc}^* moves

back towards the MPP. The rate of change of $V_{\rm dc}^*$ is set by the gain K.

The input signal $V_{\rm dc}^{**}$ represents the initial voltage reference; i.e., the starting value of the integrator. When the control system is enabled, the quantity $\Delta V_{\rm dc}$ computed by the MPPT algorithm is added to $V_{\rm dc}^{**}$, giving the actual reference of the dc link voltage $V_{\rm dc}^*$. Then, the regulation of the current i_S injected into the mains allows the dc link voltage to be controlled around the reference value. In this way, all the power coming from the PV generator is transferred to the grid. Following the reference value $V_{\rm dc}^*$ allows the PV panels to reach the maximum power operating point, where the condition $\partial p/\partial v = 0$ is satisfied.

The desired amplitude of the source current I_S^* is generated by the regulator $R(s)$, considering the dc link voltage error $V_{\rm dc} - V_{\rm dc}^*$ as the input variable. The reference value of the instantaneous source current i_S^* is generated on the basis of the amplitude I_S^*, and on the phase angle of the fundamental component of the supply voltage v_S, which is represented by the unity sinusoid $\hat{v}_S^1$ in Fig. 5 [10], [11].

The measurement of the source current is used to implement the ac current control loop. The inverter is controlled on the basis of the instantaneous current error $\Delta i_S = i_S^* - i_S$ through a predictive PWM current regulator. In particular, the inverter reference voltage v_F^* is calculated by the voltage equation written across the ac link inductance $L_{\rm ac}$, according to the block diagram represented in Fig. 1. Neglecting the resistive effects and introducing a variational model, this equation yields

$$v_F^* = v_S + \frac{L_{\rm ac}}{\Delta t}\Delta i_S \tag{14}$$

The parameter $L_{\rm ac}/\Delta t$ in (14) can be adjusted to obtain the desired regulator performance.

VI. System Performance

A. Simulation Results

The proposed MPPT algorithm, summarized in Figs. 4 and 5, has been numerically simulated by using the Simulink environment of Matlab, with reference to a single-stage converter connected to a single-phase grid, as represented in Fig. 1. The PV panels have been electrically represented by the well-known single exponential model [12], fitted on the *I–V* characteristic of a series array of ten modules of Solar Shell type SP150. The main characteristics of the PV generation system are summarized in Table I.

The performance of the power conditioning system connected to the photovoltaic array has been evaluated both in steady state and transient operating conditions determined by start up and solar irradiance variations.

In Figs. 6–9, the behavior of the control system in steady state conditions is represented. In particular, Fig. 6 shows the behavior of $\tilde{v}$ and $\tilde{p}$ around the maximum power point. Initially, $\tilde{v}$ and $\tilde{p}$ are in phase agreement, i.e., the operating point of the PV modules is on the left side of the MPP on the I–V characteristic. Subsequently, $\tilde{v}$ and $\tilde{p}$ come into in phase opposition, i.e., the operating point of the PV modules is on the right side of the MPP on the I–V characteristic. For all the operating conditions, the frequency of $\tilde{v}$ and $\tilde{p}$ is always twice that of the grid.

Fig. 7 shows the time behavior of the dc link voltage. The triangular oscillations are introduced by the hysteretic controller, whereas the sinusoidal oscillation are related to the instantaneous power exchange with the single-phase utility grid. The

TABLE I
Main Characteristics of the PV Generation System

Rated power of the PV system	P_{PV}=1.5 kW
Dc-link capacitance	C_{dc} = 2 mF
PWM carrier frequency	f_{sw} = 10 kHz
Ac-link inductor	R_{ac} = 0.1 Ω L_{ac} = 1 mH
Single phase utility grid	V_S = 127 V f = 50 Hz
Dc-link initial reference voltage	V_{dc}^{**} = 390 V
MPPT HPF: $\tau_{HPF}/(1+\tau_{HPF}s)$	$\tau_{\rm HPF}$ = 0.05 s
MPPT LPF: $1/(1+\tau_{LPF}s)$	$\tau_{\rm LPF}$ = 0.05 s
Dc-link voltage controller: PI type	K_P = 0.1 K_I = 10
Panels type (10 x, series connection)	Solar Shell SP150
Short circuit current (1000 W/m^2, 40 °C)	I_{sc} = 4.8 A
Open circuit voltage (1000 W/m^2, 40 °C)	V_{oc} = 420 V

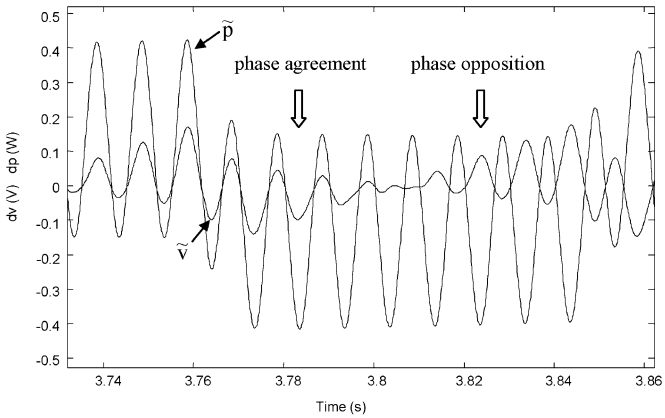

Fig. 6. Alternative components of voltage and power $\tilde{v}$ and $\tilde{p}$.

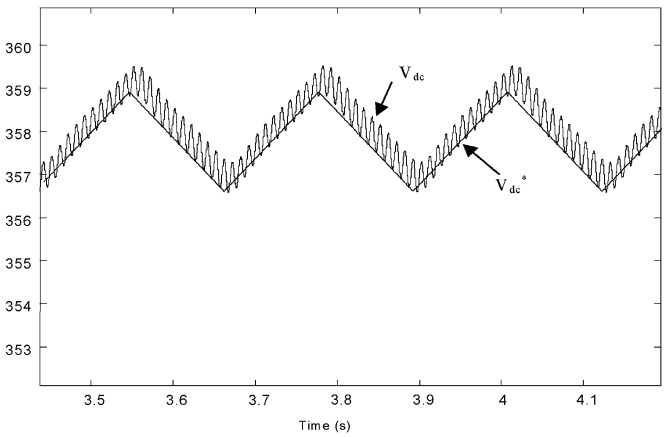

Fig. 7. DC-link voltage $V_{\rm dc}$ and dc-link reference voltage $V_{\rm dc}^*$.

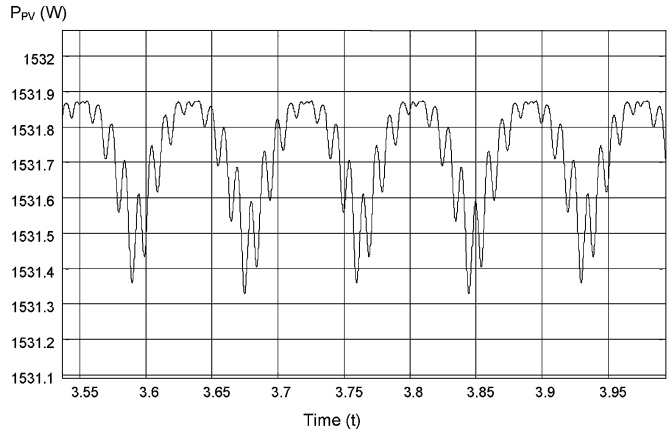

Fig. 8. Instantaneous power supplied by the PV modules.

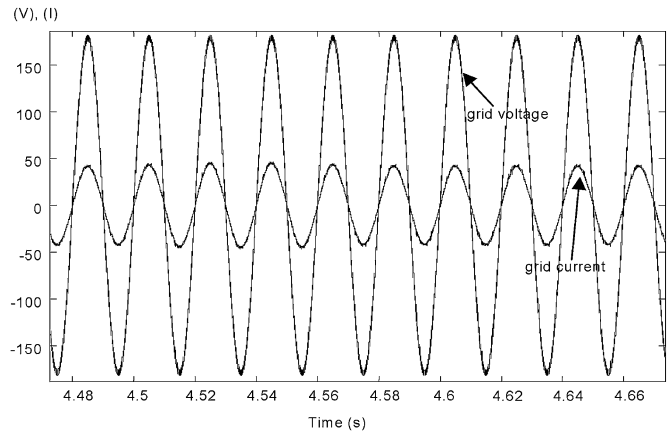

Fig. 9. Grid voltage and grid current in steady-state conditions.

oscillation amplitude is lower than 1% of the voltage at the MPP. Fig. 8 shows the small effects of these oscillations in terms of PV instantaneous power.

In Fig. 9, the voltage and the grid current are represented in steady-state conditions. As expected, the current i_S injected into the grid is exactly in phase agreement with the grid voltage v_S.

Fig. 10 shows the performance of the PV generation system in tracking the maximum power point of the PV panels during a transient of solar irradiance. From the starting operating point 1, the system reaches the MPP in 2. Then, as a consequence of a 50% reduction of the solar irradiance, the operating points move to the new MPP in 3.

B. Experimental Results

The proposed control system for a single-phase, single-stage converter has been implemented on a laboratory prototype, where the PV panels have been replaced by an electric circuit which behaves as a power generator having an output characteristic similar to that of the PV panels. The P–V characteristic of this electric source is given in Fig. 11. In this case, the open circuit voltage is 500 V, and the MPP is achieved with a dc link voltage of 250 V. A better representation of the I–V characteristic of the photovoltaic panel is proposed in [13] by introducing a

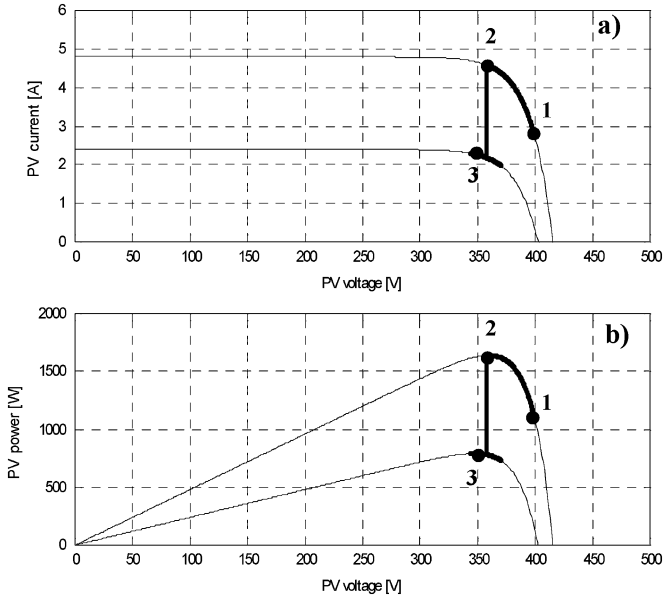

Fig. 10. Effects of a 50% solar irradiance transient. (a) PV current versus PV voltage. (b) PV power versus PV voltage.

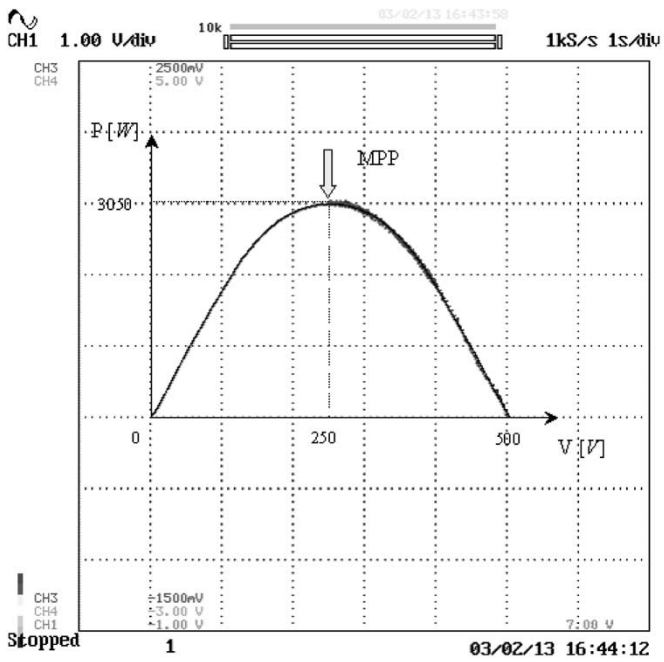

Fig. 11. P–V characteristic of the power generator replacing the PV panels.

hardware model of the PV panels, based on the power electronic model. Fig. 12 shows the steady state waveforms of voltage and current at the utility grid side. It can be noted that the resulting grid current i_S is sinusoidal and in phase agreement with the fundamental components of the grid voltage v_S, although the grid voltage has a low-order harmonic distortion.

Figs. 13 and 14 show the behavior of the proposed MPPT algorithm during the startup of the entire PV generation system. The output voltage of the power generator at the initial instant, when the converter is disabled, corresponds to the open circuit voltage (500 V).

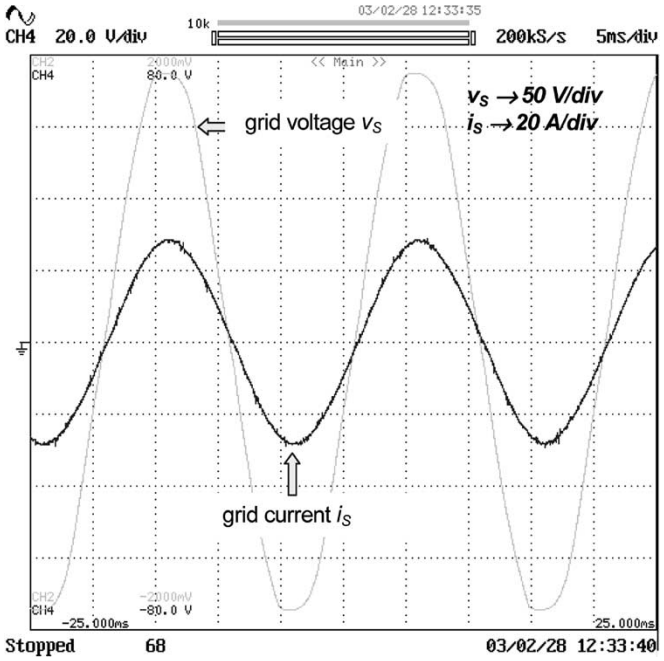

Fig. 12. Grid current i_S and grid voltage v_S in steady-state condition.

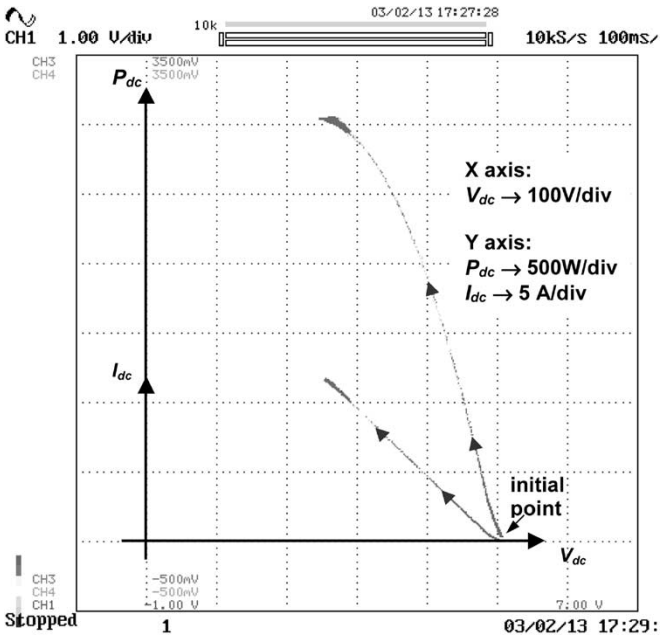

Fig. 13. P–V and I–V characteristic representing the transient during the start-up of the PV generation system.

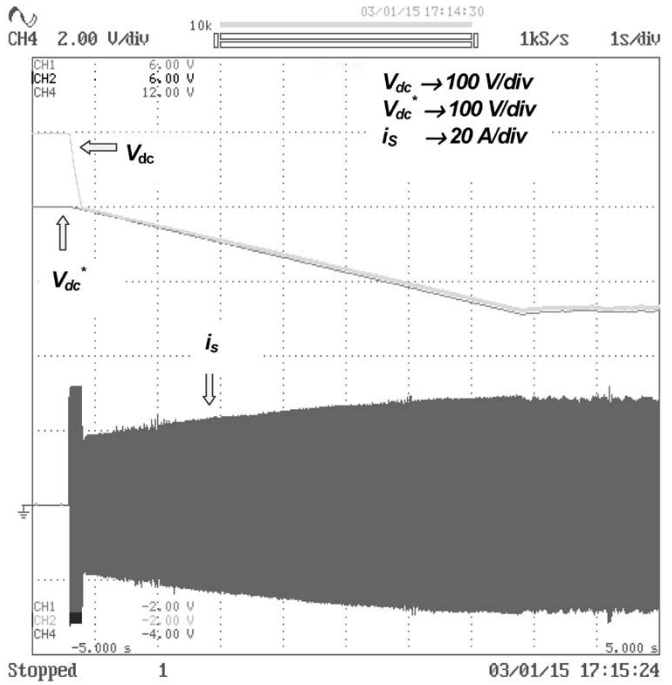

Fig. 14. $V_{\rm dc}^*, V_{\rm dc}$, and i_S during the start-up.

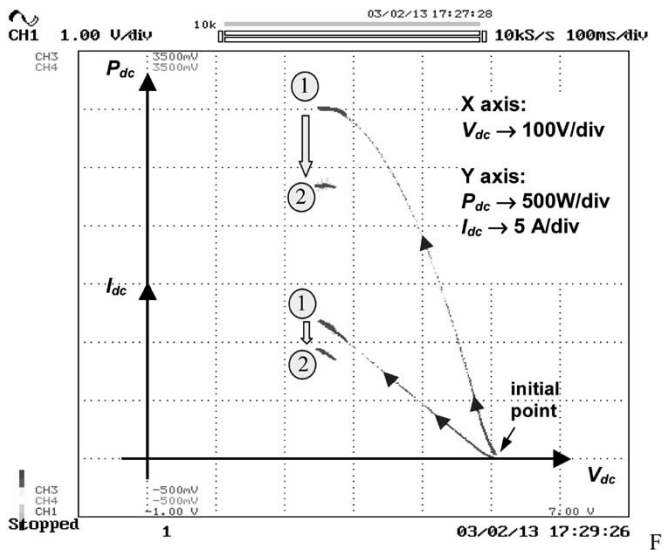

Fig. 15. P–V and I–V characteristic duringa step change of the solar irradiance.

When the system is enabled, the reference dc link voltage moves from the starting value (400 V) toward the maximum power point (250 V). During the seeking of the MPP, the dc link voltage $V_{\rm dc}$ is always close to the reference voltage $V_{\rm dc}^*$ given by the MPPT algorithm. At startup, the dc link voltage regulator guarantees a match between the reference voltage $V_{\rm dc}^*$ and the dc link voltage $V_{\rm dc}$ in about 0.2 s; then the MPP is reached in about 7 s.

Figs. 15 and 16 show the performance of the proposed MPPT algorithm in response to a step variation from 25 to 20 A of the short circuit current of the generator, corresponding to a 20% decrease in solar irradiance. The operating point moves from 1 to the new MPP in 2 in about 0.5 s. Once the new MPP is reached, only small oscillations persist around the MPP.

VII. Conclusion

A novel control strategy for single-stage converters connecting PV panels to a single-phase grid is proposed in this paper. The embedded MPPT algorithm is able to find the maximum power point by computing the sign of the PV power derivative versus voltage. This computation exploits PV current and

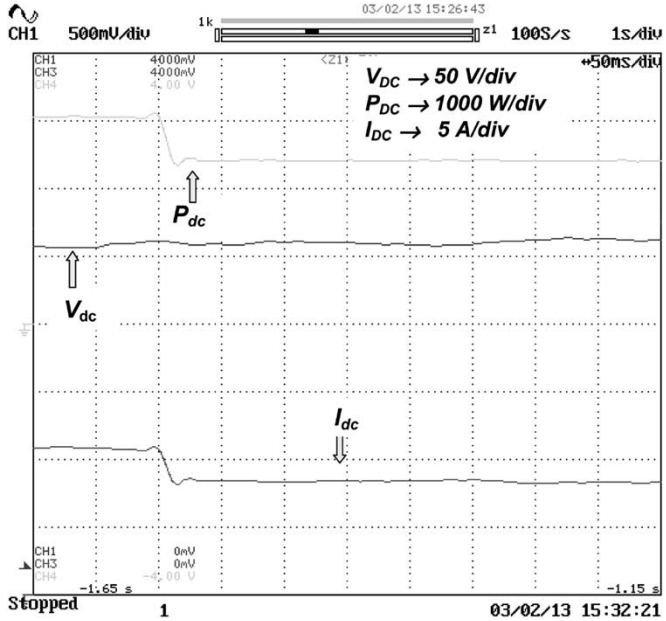

Fig. 16. Power, voltage, and current supplied by the PV generation system versus time during a transient representing a step change of the solar irradiance.

voltage oscillations, at a frequency twice than that of the grid, due to the connection of the converter with a single-phase grid. The proposed MPPT algorithm does not require knowledge of the model of the PV panels.

Once the power derivative has been computed by the MPPT algorithm, the dc link voltage regulator drives the PV panels voltage toward the MPP value. The current regulator ensures steady-state sinusoidal current and unity power factor, even in the presence of grid voltage perturbations.

The entire PV generation system has been numerically simulated and experimentally tested by a laboratory prototype.

Simulation and experimental results in both steady state and dynamic conditions have been presented. The results show good performance of the control system and confirm the effectiveness of the proposed PV generation system for any operating condition.

REFERENCES

[1] Y. C. Kuo, T. J. Liang, and J. F. Chen, "Novel maximum-power-point-tracking controller for photovoltaic energy conversion system," *IEEE Trans. Ind. Electron.*, vol. 48, no. 3, pp. 594–601, Jun. 2001.

[2] J. A. Gow and C. D. Manning, "Photovoltaic converter system suitable for use in small scale stand-alone or grid connected applications," in *Proc. Inst. Elect. Eng., Electric Power Appl.*, vol. 147, Nov. 2000, pp. 535–543.

[3] D. Casadei, G. Grandi, and C. Rossi, "Effects of supply voltage non-idealities on the behavior of an active power conditioner for cogeneration systems," in *Proc. IEEE Power Electronic Specialist Conf.*, Galway, Ireland, Jun. 2000.

[4] T. Y. Kim, H. G. Ahn, S. K. Park, and Y. K. Lee, "A novel maximum power point tracking control for photovoltaic power system under rapidly changing solar radiation," in *Proc. IEEE Int. Symp. Industrial Electronics*, vol. 2, Pusan, Korea, 2001, pp. 1011–1014.

[5] J. A. Gow and C. D. Manning, "Controller arrangement for boost converter systems sourced from solar photovoltaic arrays or other maximum power sources," in *Proc. Inst. Elect. Eng., Electric Power Appl.*, vol. 147, Jan. 2000, pp. 15–20.

[6] A. Brambilla, M. Gambarara, A. Garutti, and F. Ronchi, "New approach to photovoltaic arrays maximum power point tracking," in *Proc. 30th Annu. IEEE Power Electronics Specialists Conf.,* Charleston SC, vol. 2, Jun. 27–Jul. 1, 1999, pp. 632–637.

[7] P. Midya, P. T. Krein, R. Turnbull, R. Reppa, and J. Kimball, "Dynamic maximum power point tracker for photovoltaic applications," in *Proc. 27th Annu. IEEE Power Electronics Specialists Conf.,* Baveno, Italy, vol. 2, Jun. 23–27, 1996, pp. 1710–1716.

[8] D. L. Logue and P. T. Krein, "Optimization of power electronic systems using ripple correlation control: A dynamic programming approach," in *Proc. IEEE 32nd Annu. Power Electronics Specialists Conf.,* Vancouver, British Columbia, Canada, vol. 2, Jun. 17–22, 2001, pp. 459–464.

[9] Y. H. Lim and D. C. Hamill, "Synthesis, simulation, and experimental verification of a maximum power point tracker from nonlinear dynamics," *IEEE 32nd Annu. Power Electronics Specialists Conf.* Vancouver, British Columbia, Canada, vol. 1, pp. 199–204, Jun. 2001.

[10] D. Casadei, G. Grandi, and C. Rossi, "Dynamic performance of a power conditioner applied to photovoltaic sources," in *Proc. Power Electronic and Motion Control Conf. EPE-PEMC,* Cavtat, Croatia, Sep. 2002.

[11] G. Grandi, M. Landini, D. Casadei, and C. Rossi, "Integration of photovoltaic sources and power active filters," in *Proc. 4th ISES Europe Solar Congr.*, Bologna, Italy, Jun. 23–26, 2002.

[12] M. A. de Blas, J. L. Torres, E. Prieto, and A. García, "Selecting a suitable model for characterizing photovoltaic devices," *Renewable Energy J.*, vol. 25, no. 3, pp. 371–380, Mar. 2002.

[13] G. Grandi and G. Sancineto, "Hardware modeling of photovoltaic panels," in *Proc. ISES Solar World Congr.*, Göteborg, Sweden, Jun. 14–19, 2003.

Domenico Casadei (SM'04) was born in Rimini, Italy, in 1949. He received the Ph.D. degree (with honors) in electrical engineering from the University of Bologna, Bologna, Italy, in 1974.

He joined the Institute of Electrical Engineering, University of Bologna, in 1975. From 1975 to 1985, he was a Research Assistant, and since 1985, he has been an Associate Professor of electrical drives. He is now a Professor of electrical drives in the Department of Electrical Engineering, University of Bologna. His scientific work is related to electrical machines and drives, linear motors, maglevs, and power electronics. He has authored more than 130 papers published in technical journals and conference proceedings. His present research interests include direct torque control of induction motors, brushless motors, matrix converters, and power quality.

Dr. Casadei is a member of the IEEE Industrial Electronics and IEEE Power Electronics Societies and the Italian Electrotechnical and Electronic Association (AEI). Since 1994, he has been a member of the International Editorial Board of *Electromotion*. He is a Registered Professional Engineer in Italy.

Gabriele Grandi (M'00) was born in Bologna, Italy, in 1965. He received the M.Sc. (*cum laude*) and Ph.D. degrees from the Faculty of Engineering, University of Bologna, Bologna, Italy, in 1990 and 1994, respectively, both in electrical engineering.

Since 1995, he has been an Assistant Professor (Research Associate) in the Department of Electrical Engineering, University of Bologna. His research interests are modeling, simulation, and the design of electronic power converters, in particular, power conditioning systems. He is currently studying EMC problems related to electric power apparatus and systems (mainly switching converters and circuit models of HF components).

Claudio Rossi was born in Forlì, Italy, in 1971. He received the M.Sc. degree in electrical engineering from the University of Bologna, Bologna, Italy, in 1997. In 2001, he received the Ph.D. degree from the Department of Electrical Engineering of the same University, with a thesis entitled "Power conditioning system for the improvement of the network power quality."

Since 2000, he has been Assistant Professor of electrical machines, drives and power electronics. His present research activity is devoted to active power filters, cogeneration plants, power electronics, and drives for electric vehicles.

Dr. Rossi is a Registered Professional Engineer in Italy.